g hyperfine and superhyperfine tensors of pentavalent tungsten in polycrystalline tin dioxide

P. Meriaudeau

Laboratoire de Thermodynamique et Cinétique Chimiques, L.A. 231, Centre National de la Recherche Scientifique, Université Claude Bernard, Lyon, France

Y. Boudeville and P. de Montgolfier*

Institut de Recherches sur la Catalyse 79, boulevard du 11 Novembre 1918, 69626 Villeurbanne Cédex, France

M. Che

*Laboratoire de Chimie des Solides, Université de Paris VI, 75230 Paris Cédex 05, France [†]
and Institut de Recherches sur la Catalyse, 69626 Villeurbanne, France*

(Received 30 November 1976; revised manuscript received 1 April 1977)

Some of the tungsten ions impregnated in polycrystalline tin dioxide are found to be stabilized in the pentavalent state at substitutional positions after a heat treatment in air at 1273 K. The following ESR parameters were obtained for W^{5+} ions: $g_{xx} = 1.671$, $g_{yy} = 1.500$, and $g_{zz} = 1.732$; $A_{xx} = 48 \times 10^{-4}$ cm^{-1}, $A_{yy} = 56 \times 10^{-4}$ cm^{-1}, and $A_{zz} = 96 \times 10^{-4}$ cm^{-1}. Two superhyperfine structures were also detected. One was due to the two tin ions (a) located along the crystallographic c axis: $a_{xx} = 335 \times 10^{-4}$ cm^{-1}, $a_{yy} = 363 \times 10^{-4}$ cm^{-1}, $a_{zz} = 363 \times 10^{-4}$ cm^{-1}, and the other from the four tin ions (b) lying in the diagonal plane of the unit cell containing the four equatorial oxygens of the octahedron around the W^{5+} ion: $b_{xx} = 58 \times 10^{-4}$ cm^{-1}, $b_{yy} = 56 \times 10^{-4}$ cm^{-1}, and $b_{zz} = 52 \times 10^{-4}$ cm^{-1}. The g tensor is computed by a variational approach in the frame of the parametrized-crystal-field theory, and is in agreement with experiment. A self-consistent (on charge and configuration) extended Hückel calculation has been performed for insight on the unpaired-spin-electron molecular orbital. A contribution of the next-nearest neighbors is evidenced, but only qualitative evaluation of the superhyperfine structure is given. Delocalization of the unpaired-spin electron and local distortion of the host crystal are discussed.

I. INTRODUCTION

The ESR spectroscopy of rutile-type hosts with paramagnetic transition-metal ions has been widely studied in the past decade. (Reference 1 gives a good survey of the literature concerning these studies.) Such solids appear now to provide nice models for some real catalysts.

In recent years, tungsten has been the subject of several studies devoted both to the heterogeneous[2] and homogeneous[3] catalysis. In particular, in connection with the spillover phenomenon,[4] it was shown that a mechanical mixture of tungsten oxide WO_3 and platinum black could take up enough hydrogen at room temperature to reduce WO_3 to a hydrogen tungsten bronze H_xWO_3 with $x = 0.35$.

Despite its analogy with molybdenum oxide MoO_3, which has been extensively investigated,[5] tungsten oxide either alone or supported has hardly been looked at by ESR.[6] The main reason is that W^{5+} ions, produced by reduction, give rather broad lines which are difficult to study.

The present work, which reports on the ESR of W^{5+} ions in SnO_2, is the continuation of studies on transition-metal ions in rutile-type polycrystalline matrices[7]: Mo^{5+} in TiO_2,[8] GeO_2,[9] and SnO_2.[10,11] There has been only one previous investigation on W^{5+} ions in TiO_2 single crystals.[12]

II. EXPERIMENTAL

The amorphous tin dioxide used in this study was prepared by hydrolysis of tin tetrachloride and further neutralization with ammonia.[13]

The specific surface area was of the order of 200 m^2/g. Tungsten ions were then impregnated on SnO_2 from an ammonia solution of WO_3. After drying at 100 °C for 3 h, the samples were then fired at 1273 °K in air for 8 h. In these conditions, nitrogen impurities (such as NH_3 or NO and $NO_2{}^{2-}$)[14] were eliminated, and the structure, determined by x rays, was rutile.

Labeled tungsten was supplied as 82.63% ^{183}W-enriched WO_3. The tungsten concentration, as measured from the amount of WO_3 dissolved in ammonia, was about 10^{-2} W atoms per Sn atom.

The ESR spectra were obtained using a Varian E-3 instrument at 9.3 GHz (X band) or a Varian E-9 spectrometer at 35 GHz (Q band) with a 100-kHz field modulation.

Measurements were carried out at 77 or 300 K, and the g values were measured by comparison with DPPH (diphenyl picryl hydrazyl, $g = 2.0036$). The error on g values was estimated to be ±0.005 and those on hyperfine constants are mentioned in Table II.

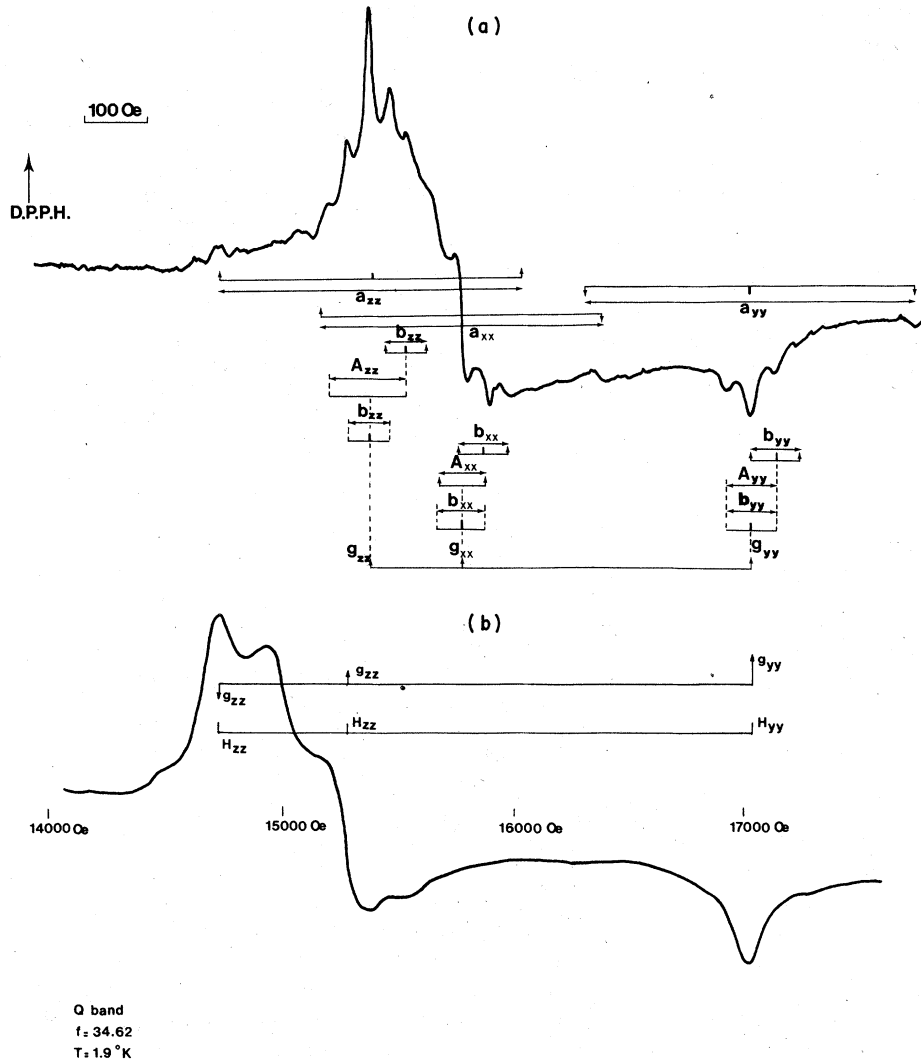FIG. 1. (a) ESR spectrum at 77 K (x-band) of W (natural isotopic abundance) doped SnO_2. The DPPH (g= 2.0036) is taken as reference and is indicated by the arrow. (b) ESR spectrum at 1.9 K (Qband) of W (natural isotopic abundance) doped SnO_2. The hyperfine and super-hyperfine lines were not detected, probably due to an increase of the individual line width[15] by the factor: frequency in Q band/frequency in X band ~ 3.8.

III. RESULTS

A. *g* tensor

Before impregnation, the white tin dioxide sample does not give any ESR signal at 77 or 300 K.

After 8 h at 1273 K in air, the natural SnO_2 : W sample gives, at 300 K, a complex ESR spectrum [Fig. 1(a)] with an orthorhombic *g* tensor, $g_1 = 1.732$, $g_2 = 1.671$, and $g_3 = 1.500$.

The Q-band signal [Fig. 1(b)] was registered at 1.9 K, as the magnitude of the signal at 77 K was not great enough to obtain a good *signal/noise* ratio; the shape of the signal was the same at 77 and 1.9 K and confirmed the *g* tensor.

The possible paramagnetic species responsible for such an ESR spectrum can be either Sn^{3+} (or F centers), W^{5+}, or W^{3+} ions. The first have been found[16] to lead to the *g* tensor $g \parallel \vec{c} = 1.905$ and

$g \perp \vec{c} = 1.876$ ($\vec{c}$ being the principal crystallographic axis) and have a very short spin-lattice relaxation time in contrast with the results reported here. Therefore, it appears that the paramagnetic species can be attributed to tungsten ions. In order to confirm this attribution, the ESR spectra of SnO_2 : W samples enriched with ^{183}W were recorded under the same conditions. The line shapes are different and are given in Fig. 2.

Because of the comparable size of W and Mo ions, we would anticipate a similar behavior of the systems Mo/SnO_2 and W/SnO_2.

On this basis, W^{3+} ions, as the origin of the ESR spectra, can be discarded, since their analogs Mo^{3+}, which have been reported mainly in[17] TiO_2 and on SiO_2,[18] exhibit a nearly isotropic *g* tensor: $g_{xx} = 1.97$, $g_{yy} = 1.94$, and $g_{zz} = 1.95$ in TiO_2 and $g_{av} = 1.928$ in SiO_2.
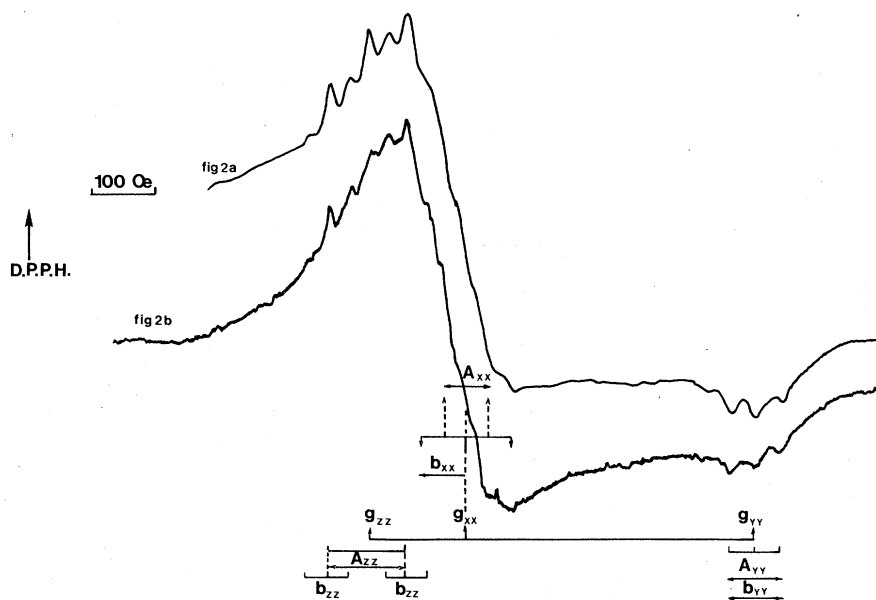
FIG. 2. (a) ESR spectrum at 77 K (X band) of ^{183}W enriched (63%) doped SnO_2. (b) ESR spectrum at 77 K (X band) of ^{183}W enriched (85%) doped SnO_2. The poor resolution of the spectra of enriched sample is probably due to the overlapping of hyperfine and superhyperfine lines.

Comparison of g tensors obtained for Mo^{5+} in various matrices and W^{5+} in TiO_2 (Table I) rather favors W^{5+} ions as the source of the ESR spectra reported here.

Table I implies that $g_1 = g_{zz}$, $g_2 = g_{xx}$, and $g_3 = g_{yy}$, which is justified when both g, a, b, and A tensors are compared (see Sec. III B). It appears that Mo^{5+} ions in SnO_2 have g components larger than those in TiO_2. In this respect, W^{5+} ions behave in a similar way.

B. Superhyperfine tensor

In order to locate the W^{5+} ions, it is necessary to consider the SnO_2 lattice which has a rutile-type structure[19] (Fig. 3). There are two equivalent Sn substitutional sites obtained by rotation of 90° about the crystallographic c axis (or y axis, both along the [001] direction). Each Sn ion is surrounded by an elongated octahedron of oxygen ions of orthorhombic symmetry. There are, in addition, four equivalent interstitial sites. Each Sn interstitial ion is surrounded by a flattened oxygen

octahedron of orthorhombic symmetry.[11]

For the substitutional site that can be considered first, the next-nearest neighbors can be divided into three groups: the (a)-, (b)-, and (c)-type Sn^{4+} cations (Fig. 3). Since[20] about 16% of the Sn nuclei have a nuclear spin $I = \frac{1}{2}$ (^{117}Sn, 7.7% with $\mu = 0.99$ nuclear magnetons, and ^{119}Sn, 8.7% with $\mu = 1.04$ nuclear magnetons), one can expect a superhyperfine (shf) structure.

For the (a)-type Sn^{4+} cations, the intensities of the superhyperfine lines can be predicted from a calculation of the probability of finding one or two ^{117}Sn or ^{119}Sn nuclei surrounding the W^{5+} substitutional site. The probability $P_n(m)$ is given by[21]

$$P_n(m) = \binom{n}{m} p^{n-m} q^m ,$$

with

$$\binom{n}{m} = \frac{n!}{m!(n-m)!} ,$$

where n refers to the total number of nearest-neighbor cation sites, m is the number of these

TABLE I. g tensors for Mo^{5+} and W^{5+} in various matrices.

	$g_{xx}[\bar{1}10]$	$g_{yy}(c$ axis) [001]	$g_{zz}[110]$	Sample	Reference
Mo^{5+}/TiO_2	1.822	1.799	1.919	powder	8
Mo^{5+}/GeO_2	1.910	1.857	1.951	single crystal	9
Mo^{5+}/SnO_2	1.891	1.835	1.923	powder	10
W^{5+}/TiO_2	1.472	1.443	1.594	single crystal	11
W^{5+}/SnO_2	1.671	1.500	1.732	powder	this work
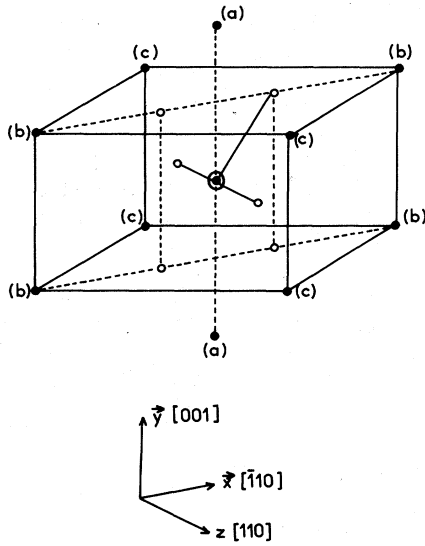
FIG. 3. SnO_2 structure with the definition of the axes and of the cations around the central ion. ●: Sn^{4+}, ○: O^{2-}, ⊖: W^{5+}.

sites occupied by ^{117}Sn or ^{119}Sn nuclei, q is the abundance of ^{117}Sn and ^{119}Sn nuclei, and p the abundance of the Sn nuclei with zero nuclear spin.

Thus the (a)-type Sn^{4+} cations lead to a shf structure which can be regarded mainly as a triplet with approximately $1;6;1$ relative intensities. The outermost lines are separated by the shf constant a due to the (a)-type Sn^{4+} cations.

Similarly, interaction of the $5d^1$ electron of W^{5+} ions with the (b)-type Sn^{4+} cations results in a shf structure leading again to a main triplet with approximatively $1;3;1$ relative intensities. The outermost lines give the shf constant b due to the (b)-type Sn^{4+} cations. The interatomic distance W-Sn(a) is only 3.2 Å, compared to the interatomic distance W-Sn(b) of 3.7 Å.[19] It is then expected that $a > b$. Interactions with (c)-type Sn^{4+} cations need not be considered because their contribution[11] is too small to be resolved.

With this approach, the ESR spectrum in Fig. 1 can be analyzed and the shf tensors a and b measured:

$$a_1 = 363 \times 10^{-4} \text{ cm}^{-1}, \quad a_2 = 335 \times 10^{-4} \text{ cm}^{-1},$$

$$a_3 = 363 \times 10^{-4} \text{ cm}^{-1}, \quad b_1 = 52 \times 10^{-4} \text{ cm}^{-1},$$

$$b_2 = 58 \times 10^{-4} \text{ cm}^{-1}, \quad b_3 = 56 \times 10^{-4} \text{ cm}^{-1}.$$

It has been shown[10,11] that, for paramagnetic transition-metal ions at substitutional sites, the largest value of the stronger superhyperfine tensor is always associated with the smallest g value along the crystallographic c axis and this is confirmed by experimental data (for a review of the

magnetic parameters see Ref. 11). This result allows us to identify g_3 with g_{yy} and a_3 with a_{yy}.

C. Hyperfine tensor

The labeling of the SnO_2:W sample with ^{183}W results in a change in the lineshape and Fig. 2 shows that now the hyperfine structure is the dominant contribution.

Since tungsten has only one naturally occurring isotope with a nuclear spin (^{183}W, $I = \frac{1}{2}$, 14.28% relative abundance) a tungsten-containing radical should show a strong central line due to the even isotopes, ($I = 0$) flanked on both sides by one satellite, each having a relative intensity of 8% of the central line. Because of the overlap with shf lines, it is difficult to distinguish them unambiguously. On the other hand, the use of tungsten 83% enriched in ^{183}W should lead to two satellites symmetrically placed around the central hyperfine line, each having an intensity about 2.4 times that of the central line. In fact, this last figure is somewhat smaller because of the linewidth dependence on M_I,[22] which causes the outermost lines to be broader than the central one. Figure 2 shows the ESR spectrum of the SnO_2:W^{5+} sample enriched with ^{183}W. The two peaks due to the hyperfine structure increase in intensity when the labeling in ^{183}W increases and the central line due to W with $I = 0$ decreases from Figs. 1, 2(a), and 2(b). The hyperfine lines are thus stronger than the shf ones. Thus, the A tensor can then be measured:

$$A_1 = 96 \times 10^{-4} \text{ cm}^{-1},$$

$$A_2 = 48 \times 10^{-4} \text{ cm}^{-1},$$

$$A_3 = 56 \times 10^{-4} \text{ cm}^{-1}.$$

Because of the association of the largest value of the hyperfine value with the largest g value along the axis of the oxygen octahedron around the transition-metal ion at substitutional site in rutile-type hosts,[11] one can now identify g_1 with g_{zz}, and A_1 with A_{zz}. With the results from Sec. II, one can thus conclude that $g_2 = g_{xx}$.

Table II summarizes the magnetic parameters for W^{5+} ions in[12] TiO_2 and SnO_2.

We have so far considered only the substitutional case. This consideration is justified because for interstitial sites,[23] the largest hyperfine value has been found, experimentally, to be associated with the smallest component of the g tensor along the axis of the flattened oxygen octahedron, while the largest g component is found along the crystallographic c axis [see Fig. 1(b) in Ref. 11 for the definition of the axes]. Obviously, our experimental data fit the substitutional case, but not the interstitial one.

TABLE II. Hyperfine and superhyperfine components of the ESR spectra of substitutional W^{5+} in TiO_2 and SnO_2.

	Hyperfine tensor			Superhyperfine tensor a			Superhyperfine tensor b			
	A_{xx}	A_{yy}	A_{zz}	a_{xx}	a_{yy}	a_{zz}	b_{xx}	b_{yy}	b_{zz}	Reference
W^{5+}/TiO_2 10^{-4} cm^{-1}	40.8	63.7	92.5	2.6	3.5	2.6				11
W^{5+}/SnO_2	62 ± 8 Oe	80 ± 3 Oe	120 ± 3 Oe	430 ± 5 Oe	520 ± 5 Oe	450 ± 5 Oe	78 ± 8 Oe	80 ± 3 Oe	64 ± 3 Oe	
10^{-4} cm^{-1}	48.3	55.9	96.9	335.2	363.8	363.6	58.4	55.9	51.7	This work

IV. THEORETICAL APPROACH

The unpaired spin electron is assumed to occupy a molecular orbital of the form

$$\psi = N^{-1/2}\left(\phi + \sum_i \mu_i \theta_i + \sum_j \nu_j \chi_j + \cdots\right),$$

where ϕ is a combination of d, s, and p orbitals of the central W ion, θ_i and χ_j are symmetry-adapted orbitals of, respectively, nearest (O) and next-nearest (Sn) neighbors (see Fig. 3).

In this part, we are interested in the connection of the ESR parameters with the different terms of this expansion and with an estimate of the localization of the unpaired electron.

A. g tensor and energy-level ordering

As a first approximation, we assume that the deviation of the g components of the ESR spectrum from the free-electron ones comes mainly from orbitals localized on the central ion, and we analyze it in terms of crystal-field splitting.

The simple electrostatic model given in Ref. 11 suggests that the ground state is $d_{x^2-y^2} - \lambda d_{z^2}$ and explains the absence of measurable interaction with (c)-type Sn^{4+} cations. However, as the spin-orbit coupling constant of W (estimated to be 5000 cm^{-1})[24] is of the same order of magnitude as the crystal field, the perturbation approach that we used before[7] for computing g tensors does not apply here. The total Hamiltonian of the central ion must be solved variationally, treating all the components on the same ground and starting from the spin orbitals of the free d^1 electron. The two lowest eigenvalues ϕ_i, labeled $|+\rangle$ and $|-\rangle$, according to their spin-majority component, are no longer of pure A_{1g} symmetry $(d_{x^2-y^2} - \lambda d_{z^2})$. The action of the Zeeman Hamiltonian on these two states lifts their degeneracy and allows one to define a g tensor.

Two of us[25] have written a FORTRAN program which enables the fitting of the g tensor of nd^1 ions in any symmetry to the experimental one, by taking the spin-orbit coupling constant ζ, the ratio of radial integrals I_2/I_4 ($I_k = \langle r^k \rangle / R^{k+1}$, R is the average distance from the central ion to the nearest neighbors) and $10Dq$ as parameters.

We have shown elsewhere,[11] that the calculation of the g tensor of substitutional nd^1 ions in rutile-type hosts necessitates to take into account at least the nearest and next-nearest neighbors of the ion under study. It turns out that there is only one way to fit the computed g tensor with the experimental one; the identification of axis 1 with z, axis 2 with x, and 3 with y, deduced from qualitative arguments, is confirmed.

Influence of the size of the model cluster on the results has been studied. If the ratio I_2/I_4 is sensitive to this size, the energy-level splitting and the ground-state wave function are not. Therefore, only the ground-state wave function $|+\rangle$ will be discussed:

$$|+\rangle = 0.983 d_{x^2-y^2} 2\alpha - 0.115 d_{z^2} \alpha - 0.0191 d_{xy}\alpha$$

$$- 0.099 d_{xz}\beta i + 0.099 d_{yz}\beta i.$$

The majority-spin component of this function is α and can be written as

$$\phi\alpha = 0.983(d_{x^2-y^2} - \lambda d_{z^2} - \epsilon d_{xy})\alpha.$$

In the first two terms, we recognize the function given by the electrostatic argument; $\lambda = 0.12$ and is close to the values obtained for substitutional V^{4+} and Mo^{5+} ions in SnO_2.[11] The β component of $|+\rangle$ comes from the mixing of the different symmetry orbitals by the spin-orbit coupling: this contribution is much larger than $d_{xy}\alpha$ contribution because d_{xy} is the most destabilized orbital. The overall computed energy-level splitting is pictured in Fig. 4.

B. Molecular orbitals

In order to get some more information on the unpaired electron localization, we have performed a SCCC EHT calculation (self-consistent in charge and configuration extended Huckel-type), on small clusters, SnO_6^{8-}, TiO_6^{8-}, and WO_6^{7-}, representative of the species under study. The different levels of approximation of the method have been discussed by Jacquier and Richardson.[26] Let us just mention that Fock matrix elements are similar to those derived by Basch and Gray[27] and Canadine and Hillier,[28] but include also the contribution of the Madelung potential of the infinite crystal. Molec-
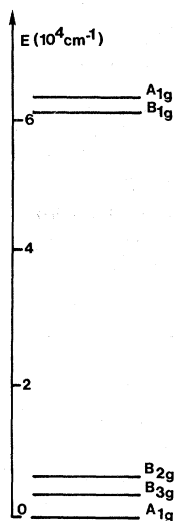
FIG. 4. d^1 energy-level splitting for $W^{5+} - SnO_2$. Energy levels are labeled according to their holohedric symmetry.

ular orbitals are expanded in terms of atomic orbitals of the neutral atoms; more details will be given elsewhere on the choice of the parameters entering into the calculation.[29]

It appears from the calculation of the electronic structure of SnO_2 that the net charge on a Sn nucleus is +3.6 (+2.6 for Ti in TiO_2). As a result, the Madelung potential experienced by the cations and the anions are, respectively, +40.03 and -22.98 eV (44.74 and -25.89 eV for TiO_2).[29] WO_6^{7-} is an open-shell system which has been dealt with in a restricted Hartree-Fock procedure by setting the occupancy of the highest occupied orbital to one. This approach is complementary of the previous one in the sense that mixing of W orbitals with first-neighbor oxygen atoms is allowed, but spin-orbit coupling is not taken into account. Interaction of WO_6^{7-} with the remaining part of the crystal is introduced via the Madelung potential of pure SnO_2 (or TiO_2). This approach allows one to compute fairly well the contribution of $5d_{z^2}$ and 6s atomic orbitals of tungsten to the molecular orbital (MO) of the ground state because admixture of $5d_{x^2-y^2}$, $5d_{z^2}$ and 6s does not occur through the spin-orbit coupling. Spin polarization is not taken into account. This consideration would be a very severe restriction if we were interested in computing accurate hyperfine interactions. The purpose of this calculation is to get a qualitative insight on the localization of the unpaired electron and to confirm the analysis of the ESR spectra.

The 25th molecular orbital has the symmetry B_{2g}, as found by the crystal-field approach,[11] because the calculation has been limited to the first coordination sphere. The 26th molecular orbital is A_{1g} and is the ground state that would be computed with a more extended cluster

$$\psi_{26} = 0.967 d_{x^2-y^2} - 0.13 d_{z^2} + 0.20[6s(W)]$$
$$- 0.02[2s(O_1) + 2s(O_2) + 2s(O_3) + 2s(O_4)]$$
$$+ 0.28[2p_x(O_1) - 2p_x(O_2) + 2p_x(O_3) - 2p_x(O_4)]$$
$$+ 0.17[2p_y(O_1) + 2p_y(O_2) - 2p_y(O_3) - 2p_y(O_4)]$$
$$+ 0.07[2p_z(O_5) - 2p_z(O_6)].$$

Several calculations on V-doped rutile have shown that the frozen orbital approximation is valid and that this orbital can be taken as a good representation of the true single electron orbital. The coefficient of the 6s(W) orbital is 0.2. For W^{5+} in TiO_2, we found the same value. As a result the isotropic part of the tungsten hyperfine tensor should be equal for $TiO_2 : W^{5+}$ and $SnO_2 : W^{5+}$. The small experimental difference (70.7×10^{-4} cm^{-1} for SnO_2 versus 66.6×10^{-4} cm^{-1} for TiO_2) could be due to a very small local distortion of the host matrix.

The λ-orbital mixing coefficient of d_z^2 is 0.13 in SnO_2 and 0.08 in TiO_2. These values are in good agreement with 0.12 and 0.07, computed by the crystal-field approach.

C. Superhyperfine contribution

The uncertainty on the choice of the parameters of the SCCC calculation discourages any computation on larger clusters which would give the delocalization of the unpaired electron on the second neighbors.

McGlynn[30] claims that the results of molecular orbital calculations do not depend much on the choice of atomic orbitals if they are balanced: atomic orbitals of O^{2-} and Sn^{4+} would lead to the same result as atomic orbitals of O and Sn, because overlaps are very similar. However, the mixing of the central-atom atomic orbitals with the next-neighbor atomic orbitals depends strongly on the charge of these species. Therefore, instead of performing detailed molecular-orbital calculations, we focus our attention on the relative magnitude of the superhyperfine contribution of a and b Sn groups.

The isotropic superhyperfine coupling constant is associated with the coefficient ν of S orbitals on the second neighbors.[1] From experimental data, we have obtained

$$\nu_a = 0.14, \quad \chi_a = \tfrac{1}{2}(S_{a_5} + S_{a_6});$$
$$\nu_b = 0.023, \quad \chi_b = (1/\sqrt{2})(S_{a_1} + S_{a_2} + S_{a_3} + S_{a_4}).$$

The ratio ν_a/ν_b is connected with the ratio of the overlap of $5d_{x^2-y^2}$ with 6s orbital of Sn_a and Sn_b atoms,[10] which has been computed to be 5.3. Comparison with $Mo^{5+} - SnO_2$ shows that the unpaired spin density on second neighbors is 40% greater

for W^{5+} than for Mo^{5+}.

The contribution of the $d_{x^2-y^2}$ orbital centered on Sn atoms is smaller than the contribution of $6s$ orbitals, because these last atomic orbitals expand farther than the first one, and the orbital mixing coefficient is probably of the order of 0.1.

V. CONCLUSIONS

The paramagnetic center detected in tungsten-doped tin dioxide is attributed to a W^{5+} ion in substitutional position in a rutile SnO_2 host, on the basis of experimental and theoretical arguments. Different aspects of the electronic structure have been discussed separately.

First, we have studied the energy-level splitting and the electronic wave function of the unpaired spin electron supposed to be localized on the tungsten nucleus. The mixing of the different representations of the D_{2h} group by the spin-orbit component of the total Hamiltonian has been evidenced.

Second, the unpaired spin electron was allowed to be delocalized on the first neighbors, but the spin-orbit interaction was neglected. The contribution of the d_{z^2} orbital to the ground-state wave function, which is governed essentially by the position of the four oxygen atoms lying in the xy plane, as computed by the MO approach and by the parametrized crystal-field approach, is not negligible.

Third, superhyperfine isotropic contributions can be rationalized in a crude molecular orbital approach; but it appears clearly that an analysis of the anisotropic component of hyperfine and superhyperfine interactions will not be meaningful at this level of approximation. However, slight modifications, with respect to the values given in Ref. 11 (Table I) of the relative values of hyperfine and superhyperfine eigenvalues of W^{5+}-SnO_2 suggest that there is a small local distortion of the lattice. Such a distortion is expected because of the excess charge of W^{5+} compared to Sn^{4+}.

Delocalization of the single electron increases in the sequence V^{4+}, Mo^{5+}, and W^{5+} when these ions are substituted in a rutile-type matrix. For the same W^{5+} ion, delocalization of the unpaired electron is greater in SnO_2 than in TiO_2.

*To whom correspondence concerning this work should be sent.

†Present address.

[1] D. P. Madacsi, R. H. Bartham, and O. R. Gilliam, Phys. Rev. B 7, 1817 (1973).

[2] P. Centola, C. Mazzochia, G. Terzaghi, and I. Pasquon, Chim. Ind. (Milan) 54, 859 (1972).

[3] G. C. Allan and A. N. Neogi, J. Catal. 16, 197 (1970). J. M. Basset, J. L. Bilhou, R. Mutin, Y. Ben Taarit, A. Theolier, and J. Bousquet, Sixth International Congress on Catalysis, London, 1976 (in press).

[4] J. E. Benson, H. W. Kohn, and M. Boudart, J. Catal. 5, 307 (1966).

[5] See, for instance, M. Che, A. J. Tench, and C. Naccache, J. Chem. Soc. Faraday Trans. I 70, 263 (1974).

[6] K. N. Spiridonov and O. V. Krylov, in Problems in Kinetics and Catalysis (Nauka, Moscow, 1975); Vol. 16.

[7] P. de Montgolfier and Y. Boudeville, Chem. Phys. Lett. 37, 97 (1976).

[8] M. Che, G. Fichelle, and P. Mériaudeau, Chem. Phys. Lett. 17, 66 (1972).

[9] T. Purcell and R. A. Weeks, Phys. Lett. A 38, 473 (1972).

[10] P. Mériaudeau, M. Che, and A. J. Tench, Chem. Phys. Lett. 31, 547 (1975).

[11] P. de Montgolfier, P. Mériaudeau, Y. Boudeville, and M. Che, Phys. Rev. B 14, 1788 (1976).

[12] T. T. Chang, Phys. Rev. 147, 264 (1966).

[13] M. Che, C. Naccache, and B. Imelik, Bull. Soc. Chim. Fr., 4791 (1968).

[14] M. Che and C. Naccache, Chem. Phys. Lett. 45, 8 (1975).

[15] G. Sperlich, P. Urban, and G. Frank, Z. Phys. 263, 315 (1973).

[16] Y. Hajimoto, E. Yamaka, N. Nagasawa, and S. Shinonoya, Phys. Lett. 23, 50 (1966).

[17] W. D. Ohlsen, Phys. Rev. B 7, 4058 (1973).

[18] R. F. Howe, J. Chem. Soc. Faraday Trans. I 71, 1689 (1975).

[19] W. H. Baur, Acta Crystallogr. 9, 515 (1956).

[20] NMR Table, 3rd ed. (Varian Associates, New York, 19xx).

[21] H. Margenau and G. M. Murphy, Mathematics of Physics and Chemistry (Van Nostrand, New York, 1956), p. 438.

[22] M. Atherton, Electron Spin Resonance (Wiley, New York, 1973), p. 327.

[23] F. Kubec and Z. Sroubek, J. Chem. Phys. 57, 1660 (1972).

[24] T. Shimizu, J. Phys. Chem. Jpn. 23, 848 (1967).

[25] Y. Boudeville and P. de Montgolfier (unpublished).

[26] B. Jacquier and J. W. Richardson, J. Chem. Phys. 63, 24 (1975).

[27] H. Basch and H. B. Gray, Inorg. Chem. 6, 639 (1967).

[28] R. M. Canadine and I. H. Hillier, J. Chem. Phys. 50, 2084 (1969).

[29] P. de Montgolfier and Y. Boudeville (unpublished).

[30] S. P. McGlynn, L. G. Vanquickenborne, M. Kinoshita, and D. G. Carroll, Introduction to Applied Quantum Chemistry (Holt, Rinehart, and Winston, New York, 1972).